FEBS Letters 583 (2009) 556–560

FEBS Letters

journal homepage: www.FEBSLetters.org

Leucine-rich hydrophobic clusters promote folding of the N-terminus of the intrinsically disordered transactivation domain of p53

L. Michel Espinoza-Fonseca

Department of Biochemistry, Molecular Biology and Biophysics, University of Minnesota, Minneapolis, MN 55455, USA
Departamento de Bioquímica, Escuela Nacional de Ciencias Biológicas, Instituto Politécnico Nacional, Prol. Carpio y Plan de Ayala, Mexico City 11340, Mexico

ARTICLE INFO

Article history:
Received 3 September 2008
Revised 8 December 2008
Accepted 24 December 2008
Available online 20 January 2009

Edited by Paul Bertone

Keywords:
Intrinsically disordered protein
p53 transactivation domain
Protein folding
Molecular dynamics simulation
Leucine-rich hydrophobic cluster

ABSTRACT

Molecular dynamics simulations have been performed on the intrinsically disordered 39-residue N-terminal transactivation domain of p53 ($p53_{1-39}$). Simulations not only revealed that $p53_{1-39}$ is natively compact, but also possesses a folded structure. Furthermore, leucine-rich hydrophobic clusters were found to play a crucial role in the formation and stabilization of the folded structure of $p53_{1-39}$. Collapsing in the sub-microsecond timescale might allow for rapid conformational turnovers of $p53_{1-39}$, necessary for its efficient transactivation activity and modulation. Fast collapsing might be the result of unique conformational landscapes, featuring several energy minima separated by small energy barriers. It is suggested that IDPs with highly specialized functions in the cell, such as transactivation, possibly display more ordered patterns than their less specialized counterparts.

1. Introduction

The existence and biological functions of intrinsically disordered proteins (IDP) have been a matter intense research for the past few years [1–11]. IDPs are characterized by a lack of folded structure and an extended conformation with high intramolecular flexibility and little secondary structure under physiological conditions [12,13]. Based on their characteristics, IDPs have been divided into two major classes: compact (molten globule-like) and extended forms [13,14]. The extended class of IDPs may exist in two different structural forms: coil-like and pre-molten globule-like. Coil-like IDPs have been found to possess very low content of secondary structure motifs and high internal flexibility, whereas pre-molten globule-like IDPs display a behavior between fully extended and molten-globular conformations and which is distinguishable by the presence of unstable secondary structure of random coil-like and molten-globule-like IDPs [13]. Coil-like and pre-molten globule-like IDPs have been found to possess motifs with marginal or transient secondary structure as well as high internal flexibility. On the other hand, molten globule-like IDPs may display a significant degree of compactness and structural order [14].

Among known IDPs, p53 has received important attention due to its key role in the cellular response to genotoxic stress by inducing cell-cycle arrest and apoptosis [15]. Its transactivation domain, located at the N-terminus of the protein, is responsible for binding proteins such as MDM2, which down-regulates the levels of p53 [16]; hence, the transactivation domain of p53 is emerging as one of the most important regions in p53 function. Nuclear magnetic resonance (NMR) [17,18], combined NMR and small-angle X-ray scattering [19], paramagnetic relaxation enhancement [20] and computer simulations [21] have shed some light on the structural features of the transactivation domain of p53. More recently, Lowry et al. proposed an ensemble of three-dimensional structures of the 71-residue transactivation domain of p53 based on distance constraints derived from paramagnetic relaxation enhancement experiments [20]. However, the authors failed to reproduce well-known features of this domain, such as the presence of a helix at positions 18–26 [17,18]. More importantly, the ensemble of structures obtained by Lowry et al. do not seem representative to the conformational states observed in the cell.

Despite the efforts in elucidating the structure and dynamics of this domain, high-resolution atomistic information of its structure and dynamics remains unclear. The need for such information is necessary to understand the internal conformational transitions experienced by p53 in the cell, their relationship with its transactivation function and modulation and its potential applications to

E-mail address: mef@ddt.biochem.umn.edu

0014-5793/$34.00
doi:10.1016/j.febslet.2008.12.060

drug design. Hence, independent all-atom molecular dynamics (MD) simulations of the extended 39-residue N-terminal transactivation domain of p53 ($p53_{1-39}$) in aqueous solution were performed to characterize its native conformational properties. MD simulations not only revealed that $p53_{1-39}$ is natively compact, but also possesses a molten globule-like, folded structure. Furthermore, leucine-rich hydrophobic clusters were found to play a crucial role in the formation and stabilization of the folded structure of $p53_{1-39}$. The functional implications of these observations are presented and discussed in this paper.

2. Materials and methods

A first set of three representative structures of the extended conformation of $p53_{1-39}$ was extracted from a 10-ns MD trajectory at 400 K in aqueous solution. The selected structures were initially found to be in an extended conformation, with some content of secondary structure. The peptides were capped with an acetyl group to the N-terminus and N-methylamide to the C-terminus and placed in a TIP3P water box with a margin of at least 25 Å between the peptide and the boundaries of the box. Such large margin was set to guarantee that the initial conformations of the peptide (with a radius of gyration of up to 20 Å) does not interact with its image, which could add a potential bias toward an artificial conformational state. Na^+ and Cl^- counterions were added to the system in order to obtain a neutral charge in the system and to produce a physiological ionic strength (~150 mM). CHARMM27 topologies and parameters were used [22,23].

MD simulations were performed using the program NAMD 2.6 [24]. For production runs, an NPT ensemble and periodic boundary conditions were imposed to the systems. The non-bonded cutoff, switching distance and non-bonded pair-list distance were set to 8, 6 and 10.5 Å, respectively. Similar cutoff, switching and pair-list distance values were recently applied to study the disorder-to-order transitions in the phosphorylation domain of the regulatory light chain of myosin, showing excellent agreement with electronic paramagnetic resonance and fluorescence data [25]. Electrostatics were modeled with the particle mesh Ewald method [26,27]. An integration timestep of 2 fs was used. Constant pressure (1 atm) and temperature (310 K) on the systems were maintained with an isotropic Langevin barostat and a Langevin thermostat. Prior production, systems were minimized by 1000 steps of conjugate gradient algorithm, warmed up for 50 ps and equilibrated for 5 ns. The total simulation time of six independent MD simulations was 0.45 μs, and snapshots were recorded every 20 ps. Analysis and visualization of the trajectories was performed using VMD [28] and CARMA [29].

3. Results and discussion

In order to extract biologically relevant conformational states of $p53_{1-39}$ from the simulations, distributions of radius of gyration values were calculated (see Fig. 1, Supplementary material). The histograms showed a bimodal behavior of $p53_{1-39}$, indicating the existence of extended and collapsed states, which are representative of the initial and final stages of the simulations, respectively. Furthermore, calculation of the radius of gyration revealed that although different initial conformational states (extended) were used a convergence to a collapsed state was observed in all MD simulations. To further demonstrate that collapsed structures represent a native, functional state of $p53_{1-39}$, 50-ns MD simulations of the most populated structure averaged over the last 10 ns of the simulations starting from an extended conformation were performed. The radius of gyration of each run showed a predominantly populated compact and relatively ordered structure in this

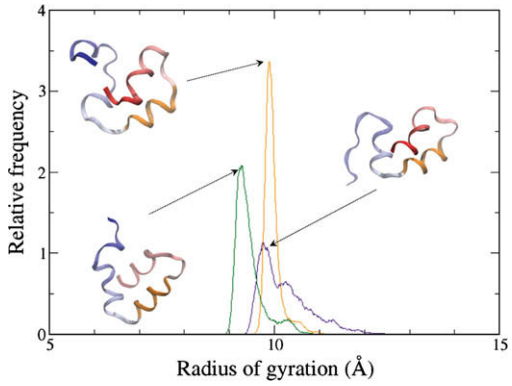

Fig. 1. Radius of gyration of the $p53_{1-39}$ starting from a compact conformation. Average structures of the domain are shown in ribbons and colored according to $p53_{1-39}$ sub-domains (blue: N-terminus; red, C-terminus; orange, α-$helix_{19-26}$).

timescale (Fig. 1). Interestingly, despite the significantly high relative frequency of the collapsed state, the radius of gyration conserved a bimodal behavior, which suggests the coexistence of both ordered and disordered segments in solution. This observation is particularly noteworthy because bimodal behavior has been suggested to be an intrinsic characteristic of IDPs in solution [20].

Structurally, the transactivation domain was found to possess a stable α-helix composed by residues Phe19-Leu26 (α-$helix_{19-26}$). The existence of this α-helix in the mostly unstructured transactivation domain has been observed in NMR experiments [17,18] and it is known for being directly involved in the binding of MDM2 to p53 [16]. The α-helix is flanked by two segments: the N-terminus (residues Met1-Gln16), mostly found as a random coil and the C-terminus (residues Asn30-Ala39), which undergoes helix-turn transitions, being turn the most predominant structural motif (see Fig. 2, Supplementary material). The presence of this structural motif in the C-terminus of $p53_{1-39}$ correlates well with the existence of a helix at position Pro36-Ala39 upon binding to the replication protein A 70 kDa DNA-binding subunit (RPA70) [30].

Cα–Cα distance maps averaged over the 50 ns of simulation of the collapsed conformations of $p53_{1-39}$ were computed in order to detect the regions that participate the folding of the peptide (Fig. 2A–C). The maps revealed two interesting features intrinsic to the structure and dynamics of this domain. First, trajectories showed the existence of a constrained C-terminus, which strongly interacts with α-$helix_{19-26}$. The N-terminus was found to be significantly more mobile compared to the rest of the peptide, although it can effectively interact with the C-terminus of the domain. These observations are in excellent agreement with NMR studies on the isolated 39-residue N-terminus of p53 [18]. In their study, Kar et al. observed a significant change in the $J_{NH-\alpha H}$ values of the α-$helix_{19-26}$ and the C-terminus upon phosphorylation at Ser15, indicating that the compactness of the central helix-C-terminus is an intrinsic characteristic of $p53_{1-39}$ [18]. Further calculation of the root-mean square deviation (RMSD) of the α-$helix_{19-26}$ and the N- and C-termini quantitatively confirmed that both central α-helix and the C-terminus are conformationally more restricted compared to the N-terminus (Table 1). The flexible nature of the N-terminus arises from its higher content of anionic residues, which prevent the segment from adopting an ordered structure via electrostatic repulsion [31].

Second, IDPs have been shown to be depleted in order-promoting amino acids (Trp, Tyr, Phe, Cys, Ile, Asn and Leu) and enriched in disorder-promoting amino acids (Pro, Glu, Lys, Ser and Gln); such amino acid content was compared to that observed in the average folded proteins in the Protein Data Bank [32]. A balance between order- and disorder-promoting amino acids confers IDPs

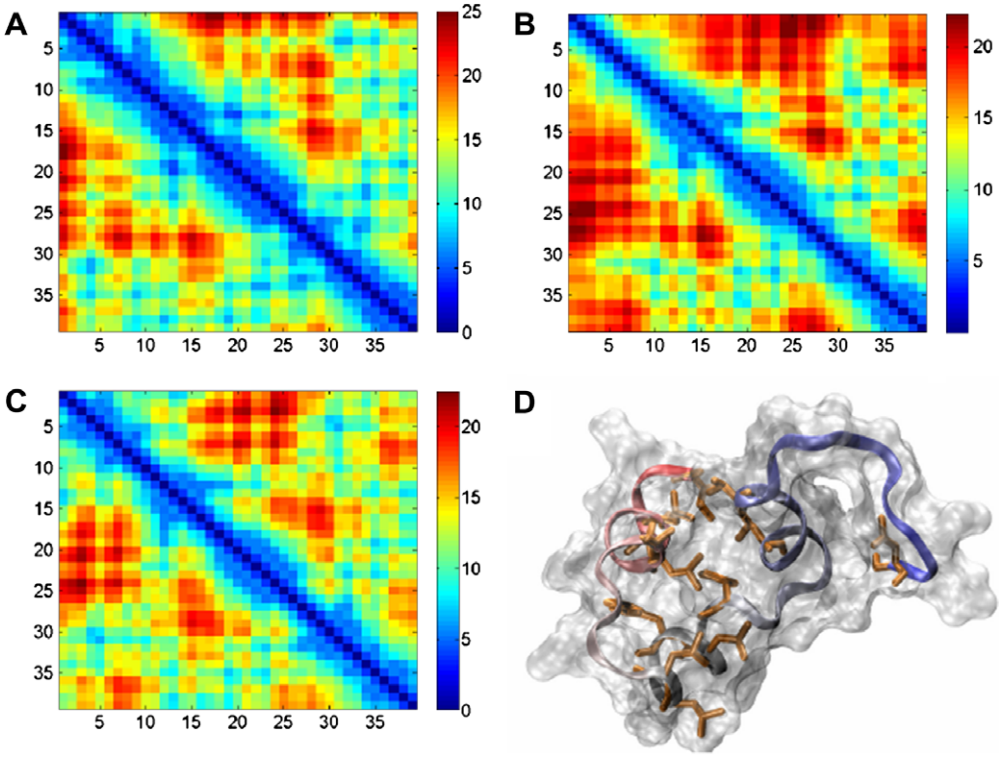

Fig. 2. (A–C) Cα–Cα distance maps calculated for the 50-ns independent simulations (distances in Å). (D) Selected structure of the N-terminus of the transactivation domain of p53.

Table 1
RMSD values calculated for the simulations starting from a compact structure of $p53_{1-39}$. RMSD values were computed using the average structure of the ensemble as a reference.

Segment	RMSD (Å)		
	Simulation 1	Simulation 2	Simulation 3
α-helix$_{19-26}$	0.22 ± 0.08	0.26 ± 0.1	0.29 ± 0.1
C-terminus (residues 30–39)	1.17 ± 0.45	3.06 ± 1.23	2.6 ± 1.07
N-terminus (residues 1–16)	1.87 ± 1.03	6.36 ± 2.67	3.28 ± 1.07
N-terminus (residues 1–10)	2.18 ± 1.28	7.96 ± 3.4	4.45 ± 2.35

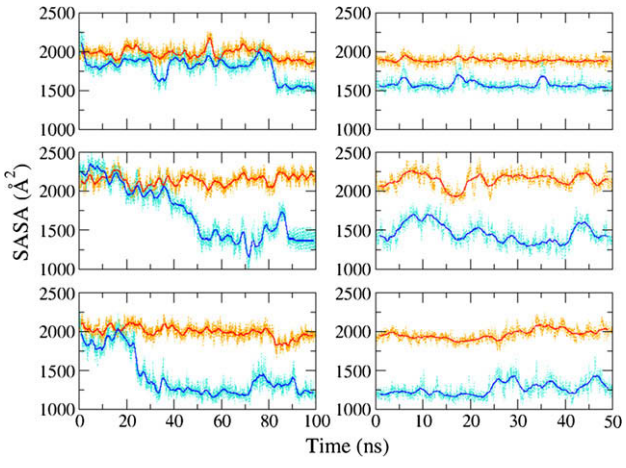

Fig. 3. Smoothed solvent-accessible surface area (SASA) of polar (red) and hydrophobic (blue) residues of $p53_{1-39}$. Left column: SASA calculated over the MD simulations starting from an extended structure of $p53_{1-39}$. Right column: SASA calculated for the three independent simulations starting from the compact structure extracted from the last 10 ns of the simulation of the extended conformations.

the ability to exist in a disorder state. Interestingly, order-promoting leucine constitutes 15.4% of the total residues of $p53_{1-39}$, a value that is significantly higher compared to the amino acid frequencies estimated for disordered proteins (5.44%) [12]. Indeed, Cα–Cα distance maps showed that leucine plays an essential role in the formation of intramolecular hydrophobic clusters. For instance, Leu32 and Leu35 from the C-terminus form hydrophobic clusters with Leu22, Leu23, Leu25 and Leu26 from the α-helix$_{19-26}$ (Fig. 2A–C). Similar hydrophobic clusters were observed between Val10 and Leu14 from the N-terminus and Leu32 and Leu35 from the C-terminus.

Recent experimental and theoretical studies on archetypal IDPs (i.e., polyglutamine, polyglycine and glycine–serine block copolypeptides) have suggested that polar IDPs prefer ensembles of collapsed structures in aqueous environments [33–35]. Similar results were observed for the glutamine/asparagine rich N-terminal domain of the yeast prion protein Sup35 [36]. Polyglycine, a useful model system for generic polypeptide backbones, was found to form compact, albeit disordered, globules in water and swollen, disordered coils in 8 M urea [33]. Together, these results have suggested that water at room temperatures is a poor solvent for generic polypeptide backbones, resulting in the peptide collapsing due to intramolecular polar forces. Given the potential relevance of these results to this study, the role of polar residues in the folding of $p53_{1-39}$ was evaluated on each individual trajectory. In order to quantitatively determine to what extend polar and hydrophobic residues participate in the folding of $p53_{1-39}$, the solvent-accessible surface area (SASA) was calculated (Fig. 3). The SASA plots revealed that polar residues do not participate in the collapsing of $p53_{1-39}$, as polar residues steadily remain exposed to solvent during the simulation time. On the contrary, SASA of hydrophobic sidechains decreases over time, clearly indicating a burial of hydrophobic residues and the formation of a collapsed state via intramolecular hydrophobic patches. Estimation of the polar and hydrophobic SASA on the 50-ns trajectories of the compact struc-

tures of the domain further demonstrated that upon collapse leucine-rich hydrophobic clusters remain stable and solvent inaccessible in this timescale. These observations, together with the Cα–Cα contact maps, demonstrate that leucine-rich hydrophobic clusters play a determinant role in the formation of a collapsed structure of $p53_{1-39}$. Experimental studies have shown that 1-anilino-8-naphtalenesulphonate (bis-ANS) is able to bind to $p53_{1-39}$ [18]. Bis-ANS, a fluorescent probe used to detect the presence of folded states in proteins, requires the formation of stable hydrophobic patches in proteins to bind [37], indicating that MD simulations correctly predicted the formation of a folded structure of the $p53_{1-39}$ via intramolecular hydrophobic clusters. Residues Phe19 and Trp23, which actively participate in the binding of p53 to MDM2, also seemed to play a marginal role in the formation and stabilization of such leucine-mediated hydrophobic clusters. However, both residues remained more exposed to solvent, feature that is intrinsic to their function in binding $p53_{1-39}$ to MDM2.

Another important issue considered in this study is the short folding timescales of the domain. By using both the radius of gyration and SASA, an average collapsing time of 52 ns was observed in three independent simulations starting from extended conformations of $p53_{1-39}$. This observation is striking, considering that ordered motifs in proteins usually fold in the microsecond timescale. Nevertheless, it is possible that a partially ordered, collapsed state (i.e., a small molten globule) can fold in the sub-microsecond time scale. Sadqi et al. measured the dynamics of protein hydrophobic collapse in the absence of competing processes [38]. Collapse was triggered with laser-induced temperature jumps in the acid-denatured form of the 40-residue protein BBL and monitored by fluorescence resonance energy transfer between probes placed at the protein ends. Interestingly, the relaxation time calculated for hydrophobic collapse was ~60 ns at 305 K, in close agreement with the collapsing timescales calculated for $p53_{1-39}$. This phenomenon may be effectively rationalized on the basis of the intrinsic nature of the free energy landscape of IDPs. Hence, fast conformational shifts between extended and collapsed (folded) states of $p53_{1-39}$ could be driven by several energy minima separated by small energy barriers in the very rugged conformational landscape. Functional sub-microsecond conformational shifts in proteins have been observed in the phosphorylation-induced disorder-to-order transitions of the regulatory light chain of smooth muscle myosin [25,39].

Tryptophan fluorescence assays on $p53_{1-39}$ have shown that Trp23 is shielded from solvent, a characteristic that is inherent to the formation of a folded conformation [18]. Following up with this observation, the distribution of number of water molecules interacting with Trp23 was calculated (see Fig. 3 and Supplementary material). It was observed that upon the formation of the stabilizing hydrophobic clusters, the number of molecules of water that interact with Trp23 decreases, in very good agreement with the fluorescence data [18]. Furthermore, structural analysis of the domain showed that, although the domain is predominantly folded, it does not adopt a spherical shape (Fig. 2D), in agreement with the experimental axial ratio of 1:7.5 [18].

Why does $p53_{1-39}$ possess a compact structure? Although the transactivation domain of p53 behaves as a *promiscuous* binder, it requires both modulation and protection mechanisms for its function. It has been shown that the motif that binds to MDM2 is the α-$helix_{19-26}$; furthermore, it has been shown that the isolated helix is unfolded or tends to disorder [18,21]. In addition, the region Pro36-Ala39 of p53 has been shown to become helical upon binding to RPA70 [30]. This suggests that the structural conservation of the linear motifs that recognize MDM2 and RPA70 (and probably other targets such as TAF or p300) is largely promoted by leucine-rich hydrophobic clusters that induce protein folding. Surprisingly, flanking regions of linear motifs have been found to be significantly enriched in leucine [40], which supports the hypothesis of hydrophobic shielding of linear motifs. Collapsing of the domain in the sub-microsecond timescale may also favor the preformation of structured binding motifs within $p53_{1-39}$, such as the RPA70 binding site. A more compact $p53_{1-39}$ would also be a result of evolution to selectively modulate its transactivation function through subtle molecular switches (i.e., phosphorylation) that produce conformational populations required for binding to specific targets. Such structural characteristic is probably connected to its particular energy landscape, which might allow for rapid conformational turnovers of this domain $p53_{1-39}$ necessary for its efficient transactivation activity and modulation, where intramolecular interactions strongly determine the "nativeness" of its functional conformational states. It is also possible that by folding, $p53_{1-39}$ protects itself from self-aggregation, which could potentially jeopardize its native functions in the cell. This hypothesis is supported by experimental evidence showing that the isolated $p53_{1-39}$ does not significantly aggregate in a 100 mM NaCl solution [18].

4. Conclusion

The results of the independent MD simulations not only confirm that the N-terminal domain of p53 is natively compact, but it also exhibits a significant degree of folded structure. Leucine-rich hydrophobic clusters appeared to play a determinant role in the formation of a folded structure of this domain. It is proposed that structure-function relationship of $p53_{1-39}$ is more complex than it has been thought, and properties such as modulation and protection against self-aggregation are intrinsic to its natively folded structure. Furthermore, observed collapsing in the sub-microsecond timescale might allow for rapid conformational turnovers of $p53_{1-39}$, necessary for its efficient transactivation activity, modulation and ubiquitination. Fast collapsing might be the result of unique conformational landscapes, featuring several energy minima separated by small energy barriers. Based on these observations, it is concluded that IDPs with highly specialized functions in the cell, such as transactivation, possibly display more ordered structural patterns than their less specialized counterparts.

Acknowledgments

The author was supported in part by grants from Barcelona Supercomputing Center and CONACYT. The author acknowledges the computer resources, technical expertise and assistance provided by the Barcelona Supercomputing Center.

Appendix A. Supplementary material

Supplementary material associated with this article can be found, in the online version, at doi:10.1016/j.febslet.2008.12.060.

References

[1] Wright, P.E. and Dyson, H.J. (1999) Intrinsically unstructured proteins: reassessing the protein structure–function paradigm. J. Mol. Biol. 293, 321–331.
[2] Dyson, H.J. and Wright, P.E. (2002) Coupling of folding and binding for unstructured proteins. Curr. Opin. Struct. Biol. 12, 54–60.
[3] Dunker, A.K., Cortese, M.S., Romero, P., Iakoucheva, L.M. and Uversky, V.N. (2005) Flexible nets. The roles of intrinsic disorder in protein interaction networks. FEBS J. 272, 5129–5148.
[4] Dyson, H.J. and Wright, P.E. (2005) Intrinsically unstructured proteins and their functions. Nat. Rev. Mol. Cell Biol. 6, 197–208.
[5] Uversky, V.N., Oldfield, C.J. and Dunker, A.K. (2005) Showing your ID: intrinsic disorder as an ID for recognition, regulation and cell signaling. J. Mol. Recognit. 18, 343–384.
[6] Receveur-Brechot, V., Bourhis, J.M., Uversky, V.N., Canard, B. and Longhi, S. (2006) Assessing protein disorder and induced folding. Proteins 62, 24–45.

[7] Bourhis, J.M., Canard, B. and Longhi, S. (2007) Predicting protein disorder and induced folding: from theoretical principles to practical applications. Curr. Protein Pept. Sci. 8, 135–149.
[8] Csizmok, V., Dosztanyi, Z., Simon, I. and Tompa, P. (2007) Towards proteomic approaches for the identification of structural disorder. Curr. Protein Pept. Sci. 8, 173–179.
[9] Radivojac, P., Iakoucheva, L.M., Oldfield, C.J., Obradovic, Z., Uversky, V.N. and Dunker, A.K. (2007) Intrinsic disorder and functional proteomics. Biophys. J. 92, 1439–1456.
[10] Uversky, V.N., Radivojac, P., Iakoucheva, L.M., Obradovic, Z. and Dunker, A.K. (2007) Prediction of intrinsic disorder and its use in functional proteomics. Meth. Mol. Biol. 408, 69–92.
[11] Uversky, V.N., Oldfield, C.J. and Dunker, A.K. (2008) Intrinsically disordered proteins in human diseases: introducing the D2 concept. Annu. Rev. Biophys. 37, 215–246.
[12] Tompa, P. (2002) Intrinsically unstructured proteins. Trends Biochem. Sci. 27, 527–533.
[13] Uversky, V.N. (2002) Natively unfolded proteins: a point where biology waits for physics. Protein Sci. 11, 739–756.
[14] Dunker, A.K. and Obradovic, Z. (2001) The protein trinity-linking function and disorder. Nat. Biotechnol. 19, 805–806.
[15] Riley, T., Sontag, E., Chen, P. and Levine, A. (2008) Transcriptional control of human p53-regulated genes. Nat. Rev. Mol. Cell Biol. 9, 402–412.
[16] Kussie, P.H., Gorina, S., Marechal, V., Elenbaas, B., Moreau, J., Levine, A.J. and Pavletich, N.P. (1996) Structure of the MDM2 oncoprotein bound to the p53 tumor suppressor transactivation domain. Science 274, 948–953.
[17] Lee, H., Mok, K.H., Muhandiram, R., Park, K.H., Suk, J.E., Kim, D.H., Chang, J., Sung, Y.C., Choi, K.Y. and Han, K.H. (2000) Local structural elements in the mostly unstructured transcriptional activation domain of human p53. J. Biol. Chem. 275, 29426–29432.
[18] Kar, S., Sakaguchi, K., Shimohigashi, Y., Samaddar, S., Banerjee, R., Basu, G., Swaminathan, V., Kundu, T.K. and Roy, S. (2002) Effect of phosphorylation on the structure and fold of transactivation domain of p53. J. Biol. Chem. 277, 15579–15585.
[19] Wells, M., Tidow, H., Rutherford, T.J., Markwick, P., Jensen, M.R., Mylonas, E., Svergun, D.I., Blackledge, M. and Fersht, A.R. (2008) Structure of tumor suppressor p53 and its intrinsically disordered N-terminal transactivation domain. Proc. Natl. Acad. Sci. USA 105, 5762–5767.
[20] Lowry, D.F., Stancik, A., Shrestha, R.M. and Daughdrill, G.W. (2008) Modeling the accessible conformations of the intrinsically unstructured transactivation domain of p53. Proteins 71, 587–598.
[21] Espinoza-Fonseca, L.M. and Trujillo-Ferrara, J.G. (2006) Transient stability of the helical pattern of region F19–L22 of the N-terminal domain of p53: a molecular dynamics simulation study. Biochem. Biophys. Res. Commun. 343, 110–116.
[22] MacKerell Jr., A.D., Bashford, D., Bellott, M., Dunbrack Jr., R.L., Evanseck, J.D., Field, M.J., Fischer, S., Gao, J., Guo, H., Ha, S., Joseph-McCarthy, D., Kuchnir, L., Kuczera, K., Lau, F.T.K., Mattos, C., Michnick, S., Ngo, T., Nguyen, D.T., Prodhom, B., Reiher III, W.E., Roux, B., Schlenkrich, M., Smith, J.C., Stote, R., Straub, J., Watanabe, M., Wiorkiewicz-Kuczera, J., Yin, D. and Karplus, M. (1998) All-atom empirical potential for molecular modeling dynamics studies of proteins. J. Phys. Chem. B 102, 3586–3616.
[23] MacKerell Jr., A.D., Feig, M. and Brooks 3rd, C.L. (2004) Improved treatment of the protein backbone in empirical force fields. J. Am. Chem. Soc. 126, 698–699.
[24] Phillips, J.C., Braun, R., Wang, W., Gumbart, J., Tajkhorshid, E., Villa, E., Chipot, C., Skeel, R.D., Kale, L. and Schulten, K. (2005) Scalable molecular dynamics with NAMD. J. Comput. Chem. 26, 1781–1802.
[25] Espinoza-Fonseca, L.M., Kast, D. and Thomas, D.D. (2008) Thermodynamic and structural basis of phosphorylation-induced disorder-to-order transition in the regulatory light chain of smooth muscle myosin. J. Am. Chem. Soc. 130, 12208–12209.
[26] Darden, T., York, D. and Pedersen, L. (1993) Particle mesh Ewald: an $N \log(N)$ method for Ewald sums in large systems. J. Chem. Phys. 98, 10089–10092.
[27] Essmann, U., Perera, L. and Berkowitz, M.L. (1995) A smooth particle mesh Ewald method. J. Chem. Phys. 103, 8577–8593.
[28] Humphrey, W., Dalke, A. and Schulten, K. (1996) VMD: visual molecular dynamics. J. Mol. Graph. 14 (33–38), 27–38.
[29] Glykos, N.M. (2006) Software news and updates. Carma: a molecular dynamics analysis program. J. Comput. Chem. 27, 1765–1768.
[30] Bochkareva, E., Kaustov, L., Ayed, A., Yi, G.S., Lu, Y., Pineda-Lucena, A., Liao, J.C., Okorokov, A.L., Milner, J., Arrowsmith, C.H. and Bochkarev, A. (2005) Single-stranded DNA mimicry in the p53 transactivation domain interaction with replication protein A. Proc. Natl. Acad. Sci. USA 102, 15412–15417.
[31] Uversky, V.N., Gillespie, J.R. and Fink, A.L. (2000) Why are "natively unfolded" proteins unstructured under physiologic conditions? Proteins 41, 415–427.
[32] Dunker, A.K., Lawson, J.D., Brown, C.J., Williams, R.M., Romero, P., Oh, J.S., Oldfield, C.J., Campen, A.M., Ratliff, C.M., Hipps, K.W., Ausio, J., Nissen, M.S., Reeves, R., Kang, C., Kissinger, C.R., Bailey, R.W., Griswold, M.D., Chiu, W., Garner, E.C. and Obradovic, Z. (2001) Intrinsically disordered protein. J. Mol. Graph. Model. 19, 26–59.
[33] Tran, H.T., Mao, A. and Pappu, R.V. (2008) Role of backbone-solvent interactions in determining conformational equilibria of intrinsically disordered proteins. J. Am. Chem. Soc. 130, 7380–7392.
[34] Crick, S.L., Jayaraman, M., Frieden, C., Wetzel, R. and Pappu, R.V. (2006) Fluorescence correlation spectroscopy shows that monomeric polyglutamine molecules form collapsed structures in aqueous solutions. Proc. Natl. Acad. Sci. USA 103, 16764–16769.
[35] Moglich, A., Joder, K. and Kiefhaber, T. (2006) End-to-end distance distributions and intrachain diffusion constants in unfolded polypeptide chains indicate intramolecular hydrogen bond formation. Proc. Natl. Acad. Sci. USA 103, 12394–12399.
[36] Mukhopadhyay, S., Krishnan, R., Lemke, E.A., Lindquist, S. and Deniz, A.A. (2007) A natively unfolded yeast prion monomer adopts an ensemble of collapsed and rapidly fluctuating structures. Proc. Natl. Acad. Sci. USA 104, 2649–2654.
[37] Das, B.K., Bhattacharyya, T. and Roy, S. (1995) Characterization of a urea induced molten globule intermediate state of glutaminyl-tRNA synthetase from *Escherichia coli*. Biochemistry 34, 5242–5247.
[38] Sadqi, M., Lapidus, L.J. and Munoz, V. (2003) How fast is protein hydrophobic collapse? Proc. Natl. Acad. Sci. USA 100, 12117–12122.
[39] Espinoza-Fonseca, L.M., Kast, D. and Thomas, D.D. (2007) Molecular dynamics simulations reveal a disorder-to-order transition on phosphorylation of smooth muscle myosin. Biophys. J. 93, 2083–2090.
[40] Fuxreiter, M., Tompa, P. and Simon, I. (2007) Local structural disorder imparts plasticity on linear motifs. Bioinformatics 23, 950–956.